

# Iron in the basal ganglia in Parkinson's disease

## An *in vitro* study using extended X-ray absorption fine structure and cryo-electron microscopy

P. D. Griffiths,<sup>1</sup> B. R. Dobson,<sup>2</sup> G. R. Jones<sup>2</sup> and D. T. Clarke<sup>2</sup>

<sup>1</sup>Academic Department of Radiology, University of Sheffield and <sup>2</sup>CLRC Daresbury Laboratory, Warrington, Cheshire, UK

Correspondence to: Professor Paul D. Griffiths, The University of Sheffield, Academic Department of Radiology, Floor C, Royal Hallamshire Hospital, Glossop Road, Sheffield S10 2JF, UK

### Summary

Iron is found in high concentration in some areas of the brain, and increased iron in the substantia nigra is a feature of Parkinson's disease. The purpose of this study was to investigate the physical environment of brain iron in post-mortem tissue to provide information on the possible role of iron in neurodegeneration in Parkinson's disease. Iron has also been implicated as the cause of signal loss in areas of high brain iron on T<sub>2</sub>-weighted MRI sequences. Knowledge of the physical environment of the brain iron is essential in interpreting the cause of signal change. Post-mortem tissue was obtained from six cases of Parkinson's disease and from six age-matched controls. Iron levels were measured using absorption spectrophotometry. Extended X-ray absorption fine structure was used to evaluate the atomic environment of iron within the substantia nigra and both segments of the globus pallidus. Cryo-electron transmission microscopy was used to probe the iron storage proteins in these

areas. Iron levels were increased in the parkinsonian nigra and lateral portion of the globus pallidus. Spectra from the extended X-ray absorption fine structure experiments showed that ferritin was the only storage protein detectable in both control and parkinsonian tissue in all areas studied. Cryo-electron transmission microscopy studies showed that ferritin was more heavily loaded with iron in Parkinson's disease when compared with age-matched controls. In summary we have shown that iron levels are increased in two areas of the brain in Parkinson's disease including the substantia nigra, the site of maximal neurodegeneration. This produces increased loading of ferritin, which is the normal brain iron storage protein. It is possible that increased loading of ferritin may increase the risk of free radical-induced damage. Differences in ferritin loading may explain regional differences in iron's effect on the T<sub>2</sub> signal.

**Keywords:** iron; Parkinson's disease; synchrotron radiation

**Abbreviation:** EXAFS = extended X-ray absorption fine structure

### Introduction

In the early part of this century, iron was shown to be in high concentration in some regions of the brain (Spatz, 1922). There is no iron in the brain at birth, but it accumulates rapidly during adolescence and early adulthood (Hallgren and Sourander, 1958), and the accumulation of iron in children can be shown by MRI (Barkovich, 1995). The basal ganglia has the highest iron concentrations in the brain, particularly the globus pallidus and substantia nigra (Hallgren and Sourander, 1958; Griffiths and Crossman, 1993). There has been renewed interest in brain iron since reports of abnormal levels of iron in various neurological diseases such as Parkinson's disease, including increased levels of iron in the substantia nigra (Dexter *et al.*, 1987; Sofic *et al.*, 1988;

Riederer *et al.*, 1989; Griffiths and Crossman, 1993). The substantia nigra pars compacta is the main site of neuronal degeneration in Parkinson's disease, but the relationship between iron deposition at this site and the aetiology and progression of Parkinson's disease is unknown. The physical state of the excess iron is not known with certainty.

We have used three techniques to investigate changes of iron content in post-mortem parkinsonian basal ganglia: absorption spectrophotometry to assay the level of iron present, extended X-ray absorption fine structure (EXAFS) to investigate the physical environment surrounding the iron, and a cryo-electron transmission microscopy study to probe storage molecules of iron.

**Table 1** Age and post-mortem delay data of the tissue used for iron concentration determination

	Mean age at death (years)	Mean post-mortem delay (h)
Control ( $n = 6$ )	$83.3 \pm 2.1$	$19.3 \pm 3.4$
Parkinson's disease ( $n = 6$ )	$83.6 \pm 2.4$	$60.0 \pm 5.9^*$

Results given are mean  $\pm$  standard deviation. \* $P < 0.01$  significantly different from control: statistics analysed by Student's  $t$  test.

## Methods

Post-mortem tissue was obtained from the Cambridge Neural Tissue Bank, Addenbrooke's Hospital, Cambridge, UK. Tissue from pathological cases had the post-mortem diagnosis of Parkinson's disease made using standard neuropathological criteria. Age-matched control tissue (from the same source) was obtained from patients with no history of neurological or psychiatric illness and showed only age-related changes histopathologically. Table 1 presents a summary of age at death and post-mortem data. Full clinical information and drug history is given in Griffiths (1998). The parkinsonian tissue was obtained from four female cases and two male cases with a mean disease duration of 7 years (range 2–16 years). The causes of death were pulmonary embolism (two), acute cardiac failure (two) and bronchopneumonia (two). All tissue was stored at  $-70^{\circ}\text{C}$  prior to analysis. No distinction was made between substantia nigra pars compacta and pars reticulata at dissection; therefore, the results presented herein are of the combined tissue.

Absorption spectrophotometry was used to measure iron levels in eight anatomical areas from six cases of Parkinson's disease and six age-matched controls. The technique has been reported previously (Griffiths and Crossman, 1993) and is summarized briefly. All glassware used in the experiment had been soaked in 8 N nitric acid for 12 h to remove any possible traces of iron. Approximately 50 mg of tissue were homogenized in 0.3 ml of double-distilled water. Triplicate 100  $\mu\text{l}$  samples were mixed with 200  $\mu\text{l}$  of 8 N nitric acid at  $95^{\circ}\text{C}$  for 4 h. The sample was made up to 2 ml with double-distilled water. A model 357 aa/ae spectrophotometer (Instrumentation Laboratory) was used with an oxygen/acetylene flame, a hollow cathode current of 8 mA, 0.3 mm bandpass and a monochromatic wavelength of 248.3 nm. The system was calibrated with two high quality iron standards of 5 and 10  $\mu\text{g/ml}$ . The sample absorption characteristics were integrated over 3 s and the first stable reading was recorded. Iron content was calculated with respect to wet weight of tissue, and the results for both groups were pooled and analysed using a two-tailed Student's  $t$  test.

## EXAFS studies

EXAFS is a technique which is capable of giving detailed structural information in many materials, but is particularly

valuable for the characterization of metal centres in biological systems. The absorption coefficient of a material is energy dependent and, if the energy is selected carefully, absorption will rise sharply as a core atom is ionized. The energy of such absorption edges is element specific. The ejected photoelectron is scattered by the neighbouring atoms and this scattering produces interference with the outgoing photoelectron wave from the absorbing atom. This interaction causes oscillations in the spectra above the absorption edge. This extended structure is called EXAFS and can be used to determine the immediate environment of the excited atom, such as inter-atomic distance and the coordination number and type of neighbouring atoms. There is already a large body of work on solution studies of iron storage proteins in which the absorption profiles have been defined. Using previous EXAFS solution work as a reference, it was hoped to identify a specific protein with the iron deposit in brain tissue.

EXAFS measurements are performed using a synchrotron radiation source, as the technique requires an intense, monochromatic source of X-rays to produce quantitative results. The experiments were performed on station 8.1 at the Synchrotron Radiation Source (SRS), Daresbury Laboratory, Warrington, UK. Samples of frozen tissue were studied from the substantia nigra and the lateral globus pallidus from six patients with Parkinson's disease and six age-matched controls (the same cases as used for absorption spectrophotometry). These anatomical regions were chosen because they are the areas of high iron deposition in Parkinson's disease.

Samples of gently homogenized tissue with a small amount of ethylene glycol were snap-frozen in liquid nitrogen, to produce solid samples without ice crystals. The samples were mounted onto a cryostat maintained at liquid nitrogen temperature. All containers that came into contact with the tissue had been soaked previously in 8 N nitric acid to remove traces of iron.

Station 8.1 contains a double-crystal  $^{220}\text{Si}$  water-cooled monochromator. The design of the crystals is such as to allow for good energy resolution ( $\sim 1$  eV at the iron K absorption edge 7.11 keV), whilst still collecting the full vertical beam. The monochromatic beam is focused on the sample by a toroidal, platinum-coated glass mirror, resulting in an estimated photon flux of  $2 \times 10^{10}$  photons/s. Spectra were collected using a 13-element solid state detector which measures the X-ray fluorescence from the sample. Ten scans of each sample were recorded in order to achieve satisfactory signal to noise.

## Cryo-electron microscopy

Frozen hydrated standards were prepared by blotting holey carbon film onto a grid which had been wetted with a diluted solution of high density horse spleen ferritin (Sigma) (Adrian *et al.*, 1984). This was snap-frozen by plunging into liquid ethane. Tissue did not come into contact with any ferrous-containing apparatus. The specimen grid was transferred to a Gatan Cryo Transfer Device (model 626) and imaged with

a Philips EM 400 at 100 kV, fitted with a Gatan anti-contaminator (model 651N), at a magnification of 43 000 and under low dose conditions. Sections of substantia nigra from six control and six Parkinson's disease cases were prepared by plunging into liquid ethane tissue which had been fixed to a sectioning stub with a 1 : 1 ethanol/propanol mixture.

Sections, 60 nm thick, were then obtained using a Reichert Ultracut S ultramicrotome equipped with a glass knife and an FCS cryo accessory at a temperature of  $-170^{\circ}\text{C}$ . Sections were transferred to 200 mesh copper folding grids and placed in the cryo transfer device before viewing in the electron microscope. The superimposed grids allow quantification of the density of distribution of iron-containing structures. Poisson fits to the distribution were made by applying the Levenberg–Marquardt method (Bevington, 1969) using the approximation:

$$P(x) = \sum_i K_i \frac{\mu^x}{x!} e^{-\mu}$$

where  $x$  is the number of particles per unit area,  $K_i$  is the coefficient of proportionality for each distribution, and  $\mu$  is the mean of each distribution. Goodness of fit was assessed by  $\chi^2$  analysis and the convergence of proportionality to unity with the minimum of parameters.

## Results

Tissue from both groups was well matched with respect to age, but the parkinsonian tissue had significantly longer post-mortem delay before temperature storage. However, the iron content of a tissue specimen should not change over the time periods concerned. Constant iron levels in control brains have been shown by our group (P. D. Griffiths, unpublished data) after 7 days storage at  $-4^{\circ}\text{C}$  and 28 days storage at  $-70^{\circ}\text{C}$ . Iron concentrations in the regions studied in Parkinson's disease and age-matched controls are presented in Table 2 as mean  $\pm$  SD. There was a wide variation of iron levels in the control telencephalic areas studied; all cortical areas had significantly lower iron concentration than the basal ganglia nuclei. The lateral globus pallidus had the highest levels, followed by the medial globus pallidus and the substantia nigra. Iron concentration was significantly raised in two areas of the parkinsonian brain: the levels were more than double those of controls in the substantia nigra and a 43% increase was observed in the lateral globus pallidus. In contrast, iron concentrations were reduced by 31% in the parkinsonian medial globus pallidus. All of these results reached statistical significance.

EXAFS spectra are shown in Figs 1 and 2. Figure 1A shows the EXAFS spectrum produced by a sample from the age-matched control substantia nigra and shows the spectrum after subtraction of the gross absorption profile, with  $k^3$  weighted absorption against  $k$ , where  $k$  is the reciprocal of the wavelength of the ejected photoelectron in  $\text{\AA}^{-1}$ .

**Table 2** Iron concentrations ( $\mu\text{g/g}$  wet weight tissue) in various anatomical sites in Parkinson's disease and control post-mortem tissue as measured by absorption spectrophotometry

Anatomical region	Control ( $n = 6$ )	Parkinson's disease ( $n = 6$ )
Putamen	119.8 $\pm$ 11.6	148.5 $\pm$ 9.9
Caudate	99.6 $\pm$ 6.6	107.7 $\pm$ 13.4
Globus pallidus (lat)	207.0 $\pm$ 9.7	295.0 $\pm$ 12.5**
Globus pallidus (med)	163.8 $\pm$ 18.3	113.7 $\pm$ 10.0*
Substantia nigra	139.8 $\pm$ 13.1	280.9 $\pm$ 21.6**
Frontal cortex (BA 10)	41.8 $\pm$ 8.2	51.4 $\pm$ 9.4
Parietal cortex (BA 39)	30.2 $\pm$ 9.3	42.7 $\pm$ 10.0
Temporal cortex (BA 21)	50.1 $\pm$ 8.5	49.3 $\pm$ 17.7

Results given are mean  $\pm$  standard deviation. BA = Brodmann area. \* $P < 0.05$  and \*\* $P < 0.01$  significantly different from controls: statistics analysed by Student's  $t$  test.

The full line is data and the dashed line is the best fit of a theoretical model. The data are modelled by the EXCURV program which calculates the theoretical spectrum in a full curved-wave formalism.

Figure 1B is a spectrum from the same sample, in which the absorption spectrum has been Fourier transformed to show the partial radial distribution function about an iron atom. Each peak represents neighbouring atoms at a specific distance. The amplitude gives information on the number of atoms at a given distance. The abscissa represents real distance in Angstroms. The least squares best fit of the model to the data shows: (i) six oxygen atoms at 1.94  $\text{\AA}$ ; (ii) 2.5 iron atoms at 2.97  $\text{\AA}$ ; and (iii) 1.7 iron atoms at 3.37  $\text{\AA}$ . (distances to  $\pm 0.1$   $\text{\AA}$ , coordination to  $\pm 0.2$ ). The split iron shell (at 3.0 and 3.4  $\text{\AA}$ ) is a characteristic of ferritin, as is the 6-oxygen and 4-iron coordination (Mackle *et al.*, 1991, 1993).

Figure 2A and B shows the equivalent spectra from parkinsonian substantia nigra. The fitting parameters are very similar to the control cases: (i) six oxygen atoms at 1.95  $\text{\AA}$ ; (ii) 2.4 iron atoms at 3.00  $\text{\AA}$ ; and (iii) 1.7 iron atoms at 3.38  $\text{\AA}$ . The spectra for the parkinsonian and control globus pallidus were similar to those from the substantia nigra. Therefore, in both regions and in both conditions, the only focus of iron detectable by this method was ferritin.

Electron-dense particles were observed in the substantia nigra and globus pallidus in Parkinson's disease and control tissue by cryo-electron transmission microscopy. These were similar in form to those shown in the horse spleen ferritin standards. In view of this finding and the results of EXAFS experiments, the electron-dense particles were equated with ferritin. Analysis of the density of distribution of ferritin showed that the number of ferritin cores was statistically higher in Parkinson's disease tissue (see Table 3). There were differences in ferritin core clustering between Parkinson's disease and age-matched controls. The probability distribution curves for ferritin cores could not be fitted by a simple

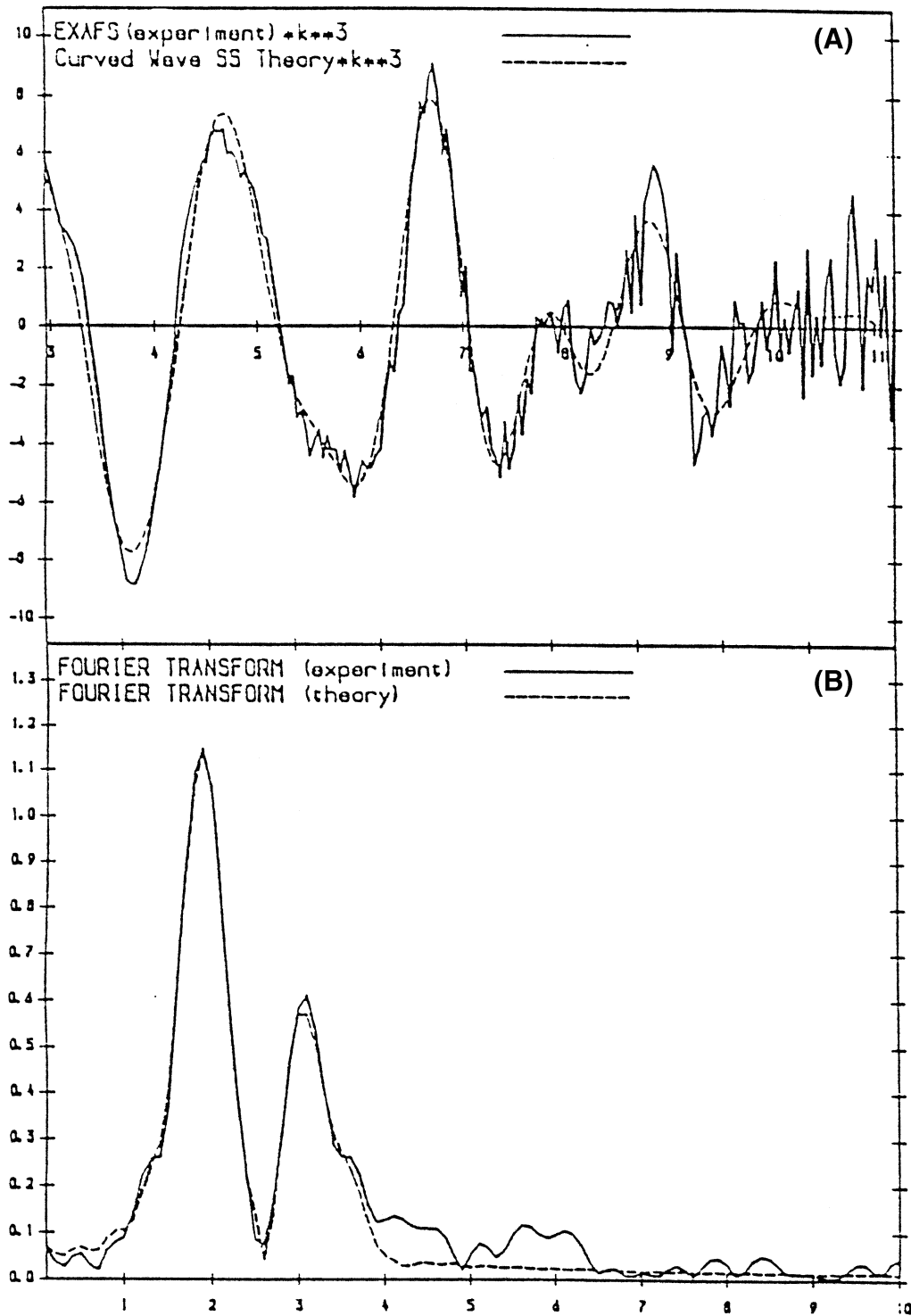


**Fig. 1** Extended X-ray absorption fine structure spectra from an aged control sample of substantia nigra. (A) Absorption after subtraction of the gross absorption profile ( $k^3$  weighted absorption against  $k$ , where  $k$  is the reciprocal of the photoelectron wavelength). The solid line is the actual data and the dashed line is the best fit of a theoretical model. (B) The spectrum after Fourier transformation. Each peak represents neighbouring atoms at a given distance. The spectra are typical of ferritin.

Poisson distribution, implying a non-random distribution. Attempts to fit the data with sums of Poisson parent functions were more successful. Three Poisson terms were required to

fit the control tissue and four Poisson terms to fit the Parkinson's disease tissue. This indicates a greater degree of subcellular clustering in the parkinsonian tissue.

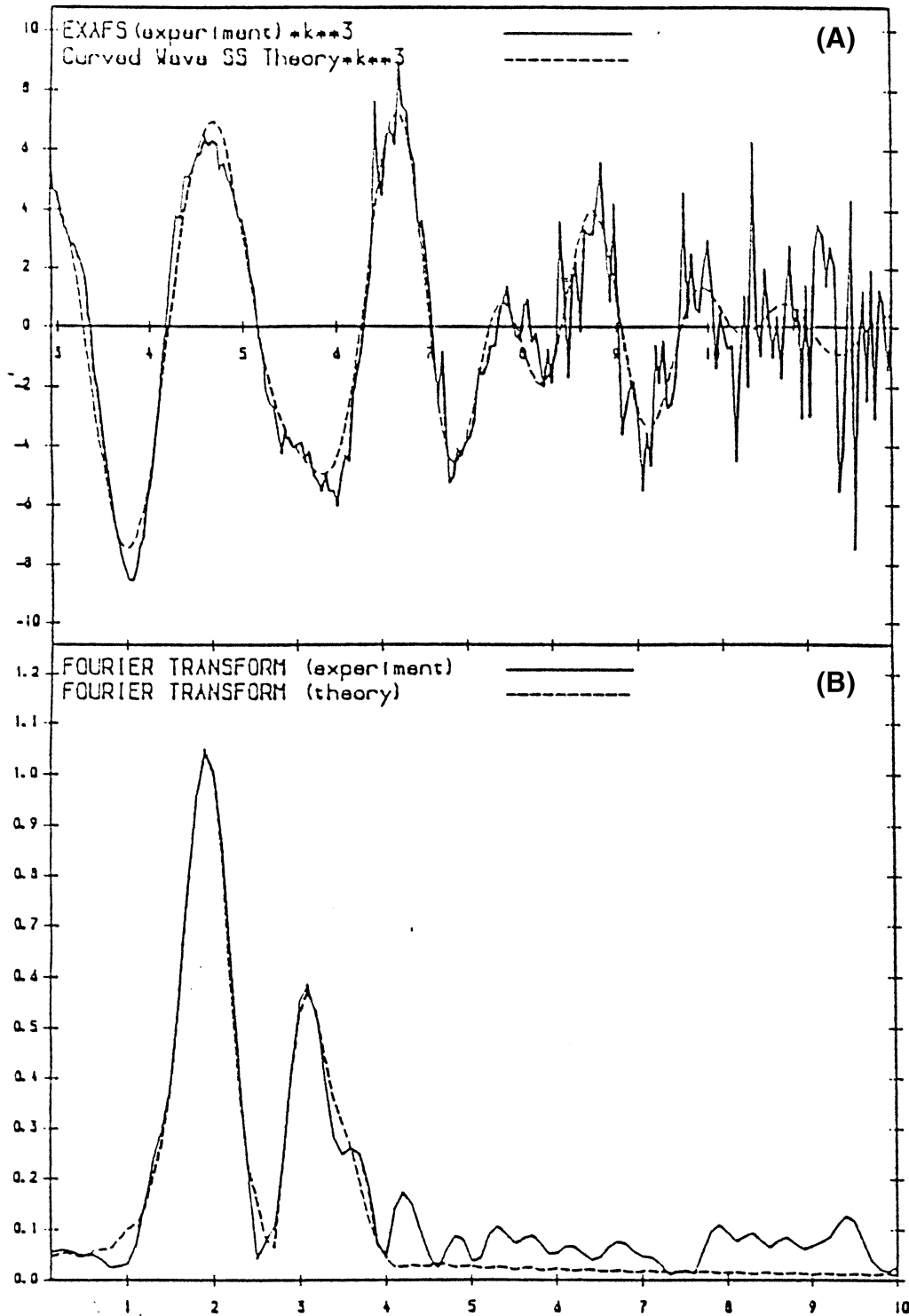


**Fig. 2** Extended X-ray absorption fine structure spectra from parkinsonian nigra. (A) Absorption after subtraction of the gross absorption profile and (B) the Fourier transformation. The spectra are not significantly different from those of the control tissue, implying that ferritin is the only definable iron-containing structure.

## Discussion

The distribution and concentration of iron demonstrated in aged control brains in this study are comparable with those described by other authors (Hallgren and Sourander, 1958;

Dexter *et al.*, 1987). The highest levels of iron are found within the globus pallidus and substantia nigra. It is not known with certainty how iron enters the brain, as  $\text{Fe}^{2+}$  and  $\text{Fe}^{3+}$  ions are not able to cross the blood-brain barrier.

**Table 3** The results of cryo-electron microscopy studies

	No. of ferritin cores/ 0.003 $\mu\text{m}^3$ tissue
Control tissue ( $n = 6$ )	$2.95 \pm 0.21$
Parkinson's disease tissue ( $n = 6$ )	$6.50 \pm 0.35^*$

The results, given as mean  $\pm$  standard deviation, show increased numbers of ferritin cores in the substantia nigra of Parkinson's disease tissue compared with controls ( $*P < 0.01$  Student's  $t$  test).

Transferrin-binding sites have been demonstrated in the brain in both rodents and humans (Hill and Switzer, 1984; Kalaria *et al.*, 1992; Griffiths and Crossman, 1996) and this is the most likely means of entry. Comparison of the distribution of transferrin-binding sites and iron concentration has shown a mismatch (Hill and Switzer, 1984; Griffiths and Crossman, 1996). Regions of high iron levels have low or no transferrin-binding sites (e.g. globus pallidus and substantia nigra), whereas grey matter regions with low levels of iron have a high density of transferrin-binding sites (e.g. cerebral cortex). On the basis of this distribution, Hill suggested that transferrin-binding sites may be located on neuronal bodies and the internalized iron may be transported down axons to remote sites.

The cellular and subcellular distributions of iron are also uncertain. Small quantities of iron are found in enzyme systems, e.g. tyrosine hydroxylase and monoamine oxidase. In the rodent, iron appears to be contained in oligodendrocytes (Hill and Switzer, 1984) and, in the midbrain, most iron is sited in the oligodendrocytes of the substantia nigra pars reticulata (Hill and Switzer, 1984). Many authors have described ferritin as the main iron storage compound (Riederer *et al.*, 1989; Dexter *et al.*, 1991), and ferritin was the only detectable iron-containing compound found in Parkinson's disease and age-matched controls in the present study. Ferritin is a storage protein which consists of a spherical shell comprising 24 subunits of apoferritin.

The average consistency of the inner iron micellar core is  $(\text{FeO-OH})_8 \text{FeO-OPO}_3\text{H}_2$ , and this core can have a variable number of iron atoms (mostly as  $\text{Fe}^{3+}$ ) associated with it, up to a maximum of  $\sim 4500$ . It is known that high iron levels may promote ferritin production within peripheral cells (Dexter *et al.*, 1991), and it is possible that this mechanism occurs within the central nervous system. Rutledge *et al.* (1987) compared the distribution of ferric iron in post-mortem brains demonstrated by Perls' staining method with the estimated decrease of  $T_2$  relaxation times from T2W MRI examinations. On the basis of this observation, the authors suggested that iron was responsible for the decrease in  $T_2$  relaxation. The anatomical match was close but not perfect; for example, the components of the striatum, i.e. the putamen and caudate, which have a moderately high concentration of iron, showed little decrease in  $T_2$  relaxation when compared with the adjacent globus pallidus. The theory that iron is responsible for the  $T_2$  signal loss has been challenged by

some authors and appears to be far more complicated than originally thought. Knowledge of the molecular storage form is essential to interpreting the MRI data (Schenk *et al.*, 1990). Iron has been found in abnormal concentrations in a variety of neurological disorders, including multiple sclerosis, Hallervorden-Spatz disease and tardive dyskinesia, and there is a considerable body of evidence that there is an abnormality of iron distribution in Parkinson's disease.

The consistent finding is increased iron levels within the substantia nigra of Parkinson's disease (Dexter *et al.*, 1987; Sofic *et al.*, 1988; Riederer *et al.*, 1989), and this finding is confirmed in this study. We also report divergent changes of iron concentration in the globus pallidus. This finding has not been described by other workers, possibly because previous studies have not investigated the lateral and medial segments of the globus pallidus separately. It is difficult to explain the divergent changes of iron within the globus pallidus, but an interested reader is directed to Hill and Switzer (1984).

The increased levels of iron within the substantia nigra of Parkinson's disease are potentially more important because this is the site of the major neurodegenerative process in Parkinson's disease. It is possible that the high concentration of iron found in the parkinsonian nigra results purely from contraction of the nigral neuropil due to the degenerative process. However, the cell types involved in the degenerative scarring process are astrocytes, which do not concentrate iron (Hill and Switzer, 1984). This has led many authors to speculate on a primary role of iron in the nigral cell loss and prompted a large body of work investigating the nature of the iron deposition within the parkinsonian nigra. High iron levels have been demonstrated in the oligodendrocytes of the substantia nigra pars compacta in Parkinson's disease (Dexter *et al.*, 1989, 1991), although other workers have shown increased iron levels in the dopaminergic neurons of the pars compacta.

It is thought that most of the intracellular iron is stored as  $\text{Fe}^{3+}$  within ferritin. The results of our present EXAFS study, in both Parkinson's disease and control brain tissue, reveal that the partial radial distribution about the iron atoms is identical and matches the previously published ferritin spectra, and we were not able to show any other iron storage form using EXAFS. Thus, we believe that iron in the human brain is stored as ferritin.

Ferritin levels have been measured in the substantia nigra in Parkinson's disease and were found to be raised in one study (Riederer *et al.*, 1989), but were shown to be reduced in the parkinsonian substantia nigra and globus pallidus in another (Dexter *et al.*, 1991).

The results of our cryo-electron transmission microscopy study show that there is an increased density of ferritin cores within the substantia nigra of parkinsonian tissue when compared with age-matched controls and that ferritin molecules are more heavily loaded with iron. This is an important finding because of the possible role of iron in initiating neurodegeneration. Although iron is present

normally in the brain, it is known that modest increases in iron concentration may cause neuronal damage. A possible mechanism for this is the generation of free radicals (Halliwell and Gutteridge, 1985). Free radicals are normally generated in cells and are essential in aerobic respiration; however, the concentrations and extent must be closely controlled. Increased levels of free radicals can arise from a reduction in the systems which usually nullify their effects (free radical scavengers) or by overproduction. There is accumulating evidence that the substantia nigra in Parkinson's disease may be particularly susceptible to this type of insult because of excessive free radical formation and a deficiency in the free radical scavenging mechanisms.

Iron is important in this process because its multivalent nature allows acceptance of electrons during the formation of free radicals; however, the role of iron in the pathogenesis of Parkinson's disease is uncertain (for a review, see Adams and Odunze, 1991). Chelated intracellular iron will cause cell death by the production of free radicals, and some authors have suggested that iron may exist in a chelated form in neurons, although we were unable to confirm this in the present study. The storage of iron within ferritin may act as a protective mechanism, but heavily loaded ferritin may still produce free radicals. It is possible that the increased loading of ferritin in Parkinson's disease shown in this study provides an environment that encourages free radical generation and hence neuronal damage.

In summary, we have described experiments which show that iron is increased in the parkinsonian brain and that the iron is stored as ferritin. In Parkinson's disease, the ferritin molecules are more heavily loaded with iron when compared with age-matched controls, and this may predispose to free radical-based neuronal damage.

## Acknowledgements

The authors would like to thank the Director of the Synchrotron Radiation Source for access to their facility and to the many members of staff who helped with this work.

## References

- Adams JD Jr, Odunze IN. Oxygen free radicals and Parkinson's disease. [Review]. *Free Radic Biol Med* 1991; 10: 161–9.
- Adrian M, Dubochet J, Lepault J, McDowell AW. Cryo-electron microscopy of viruses. *Nature* 1984; 308: 32–6.
- Barkovich AJ. Normal development of the neonatal and infant brain, skull and spine. In: Barkovich AJ, editor. *Paediatric neuroimaging*. 2nd edn. New York: Raven Press; 1995. p. 9–54.
- Bevington PR. *Data reduction and error analysis for the physical sciences*. New York: McGraw-Hill; 1969.
- Dexter DT, Wells FR, Agid F, Agid Y, Lees AJ, Jenner P, et al. Increased nigral iron content in postmortem parkinsonian brain [letter]. *Lancet* 1987; 2: 1219–20.
- Dexter DT, Wells FR, Lees AJ, Agid F, Agid Y, Jenner P, et al. Increased nigral iron content and alterations in other metal ions occurring in brain in Parkinson's disease. *J Neurochem* 1989; 52: 1830–6.
- Dexter DT, Carayon A, Javoy-Agid F, Agid Y, Wells FR, Daniel SE, et al. Alterations in the levels of iron, ferritin and other trace metals in Parkinson's disease and other neurodegenerative diseases affecting the basal ganglia. *Brain* 1991; 114: 1953–75.
- Griffiths PD. *Alterations in neurotransmitter receptors and iron content in Parkinson's disease and Alzheimer's disease*. [PhD thesis]. Manchester: University of Manchester; 1998.
- Griffiths PD, Crossman AR. Distribution of iron in the basal ganglia and neocortex in postmortem tissue in Parkinson's disease and Alzheimer's disease. *Dementia* 1993; 4: 61–5.
- Griffiths PD, Crossman AR. Autoradiography of transferrin receptors in the human brain. *Neurosci Lett* 1996; 211: 53–6.
- Hallgren B, Sourander P. The effect of age on the non-haemin iron in the human brain. *J Neurochem* 1958; 3: 41–51.
- Halliwell B, Gutteridge JM. Free radicals and antioxidant protection: mechanisms and significance in toxicology and disease. *Hum Toxicol* 1988; 7: 7–13.
- Hill JM, Switzer RC 3d. The regional distribution and cellular localization of iron in the rat brain. *Neuroscience* 1984; 11: 595–603.
- Kalaria RN, Sromek SM, Grahovac I, Harik SI. Transferrin receptors of rat and human brain and cerebral microvessels and their status in Alzheimer's disease. *Brain Res* 1992; 585: 87–93.
- Macke P, Garner CD, Ward RJ, Peters TJ. Iron K-edge absorption spectroscopic investigations of the cores of ferritin and haemosiderins. *Biochim Biophys Acta* 1991; 1115: 145–50.
- Macke P, Charnock JM, Garner CD, Meldrum FC, Mann S. Characterization of the manganese core of reconstituted ferritin X-ray absorption spectroscopy. *J Am Chem Soc* 1993; 115: 8471–2.
- Riederer P, Sofic E, Rausch WD, Schmidt B, Reynolds GP, Jellinger K, et al. Transition metals, ferritin, glutathione, and ascorbic acid in parkinsonian brains. *J Neurochem* 1989; 52: 515–20.
- Rutledge JN, Hilal SK, Silver AJ, Defendini R, Fahn S. Study of movement disorders and brain iron by MR. *Am J Roentgenol* 1987; 149: 365–79.
- Schenck JF, Mueller OM, Souza SP, Dumoulin CL. Magnetic resonance imaging of brain iron using a 4 Tesla whole-body scanner. In: Frankel RB, Blakemore RP, editors. *Iron biominerals*. New York: Plenum Press; 1990. p. 373–85.
- Sofic E, Riederer P, Heinsen H, Beckmann H, Reynolds GP, Hebenstreit G, et al. Increased iron (III) and total iron content in post mortem substantia nigra of parkinsonian brain. *J Neural Transm* 1988; 74: 199–205.
- Spatz H. *Über die Eisennachweise im Gehirn, besonders in Zentren des extrapyramidal-motorischen Systems. Teil I. Z Ges Neurol Psychiat* 1922; 77: 261–390.

Received April 14, 1998. Revised September 17, 1998.

Accepted November 30, 1998